Organic Geochemistry 141 (2020) 103974

Contents lists available at ScienceDirect

Organic Geochemistry

journal homepage: www.elsevier.com/locate/orggeochem

Identification of a novel undecamethylhenicosane and three oxygenated precursors in a Maoming Basin shale, China

Jing Liao [a,b], Hong Lu [a,*], Qiao Feng [b], Youping Zhou [c,*], Quan Shi [d], Ping'an Peng [a], Guoying Sheng [a]

[a] State Key Laboratory of Organic Geochemistry, Guangzhou Institute of Geochemistry and Institutions of Earth Science, Chinese Academy of Sciences, Guangzhou 510640, China
[b] Shandong Provincial Key Laboratory of Depositional Mineralization and Sedimentary Minerals, Shandong University of Science and Technology, Qingdao 266000, China
[c] Isotopomics in Chemical Biology & Shaanxi Key Laboratory of Chemical Additives for Industry, School of Chemistry & Chemical Engineering, Shaanxi University of Science & Technology, Xi'an 710021, China
[d] State Key Laboratory of Heavy Oil Processing, China University of Petroleum, Beijing 102249, China

ARTICLE INFO

Article history:
Received 16 May 2019
Received in revised form 26 December 2019
Accepted 2 January 2020
Available online 7 January 2020

Keywords:
C_{32} botryococcane
C_{32} botryococcanal
C_{31} botryococcanol
NMR
Bacterial degradation
Maoming Basin

ABSTRACT

Further to our recent identification of a C_{33} botryococcane, a C_{33} botryococcan-24-one and two C_{31} botryococcanes (2,3,6,7,10,12,15,16,19,20-decamethylhenicosanes: C_{31} DMHs) with a methyl group β-positioned to the sole quaternary carbon in the skeleton in a sediment sample from the Maoming Basin, we report the NMR-based structural identification of a new C_{32} botryococcane (2,3,6,7,10,10,12,15,16,19,20-undecamethylhenicosane: C_{32} UMH), and MS-based structural identification of a C_{32} botryococcanal (C_{32} UMH-al) and two C_{31} epimeric botryococcanols (C_{31} DMH-ols) in the same sediment sample after trimethylsilylation. These three oxygenated botryococcanoids are speculated to possess the same β-positioned methyl group (to the sole quaternary carbon).

We propose that the C_{32} UMH-al and two epimeric C_{31} DMH-ols are degradation products of the C=C double bond in the ethenyl group connected to the sole quaternary carbon in their biological precursor C_{33} botryococcene with a unique β-positioned methyl group (to the quaternary carbon), and are geochemical precursors for the C_{32} UMH and previously identified C_{31} DMHs, respectively. Since it is known that abiotic degradation (photo-mediated or autoxidation) preferentially acts on the internal double bond while sedimentary bacteria preferentially degrade the terminal double bond, our finding of a degraded terminal C24-25 double bond and an intact internal double bond (at C11-12) is indicative of bacterially mediated degradation. A detailed bacterially mediated degradation pathway is proposed to explain the formation of C_{31}–C_{33} botryococcanes and their oxygenated derivatives.

1. Introduction

Botryococcanes are geochemically saturated botryococcenes known to be derived only from race B of the freshwater unicellular green microalga *Botryococcus braunii* (Maxwell et al., 1968; Moldowan and Seifert, 1980; McKirdy et al., 1986; Volkman, 2014). They therefore carry useful biological, depositional environmental and geological age information (Philp and Lewis, 1987; Guy-Ohlson, 1992; Volkman, 2014). In a Chinese Maoming Basin sediment sample, Liao et al. (2018a) discovered an abundant odd-carbon-numbered C_{33} botryococcane with a unique skeleton containing a methyl group positioned β- to the sole quaternary carbon and proposed a new bio- and geochemical pathway for its occurrence. Shortly after that, two C_{31} botryococcanes (DMHs: decamethylhenicosanes, Liao et al., 2018b) with the same unique carbon skeleton of the C_{33} botryococcane were also reported to occur in the same sediment sample (Liao et al., 2018a) (Fig. 1a). In the total ion chromatogram (TIC) of the saturated fraction examined by Liao et al. (2018a, 2018b) a prominent peak was observed to elute between the two C_{31} DMHs and C_{33} botryococcane. The low-resolution mass spectrum (Fig. 1b) was characteristic of a botryococcane. To ascertain its carbon number and structure, we purified this compound by preparative gas chromatography and structurally characterised it by 2D NMR. The results indicated it was indeed a C_{32} botryococcane with the same unique skeleton as the C_{31} and C_{33} botryococcanes.

* Corresponding authors at: State Key Laboratory of Organic Geochemistry, Guangzhou Institute of Geochemistry and Institutions of Earth Science, Chinese Academy of Sciences, 511 Kehua Street, Tianhe District, Guangzhou 510640, China, (H. Lu), Isotopomics in Chemical Biology & Shaanxi Key Laboratory of Chemical Additives for Industry, School of Chemistry & Chemical Engineering, Shaanxi University of Science & Technology, Xianqing Av, Weiyang District, Xi'an 710021, China (Y. Zhou).

E-mail addresses: luhong@gig.ac.cn (H. Lu), youping.zhou@sust.edu.cn (Y. Zhou).

https://doi.org/10.1016/j.orggeochem.2020.103974
0146-6380/

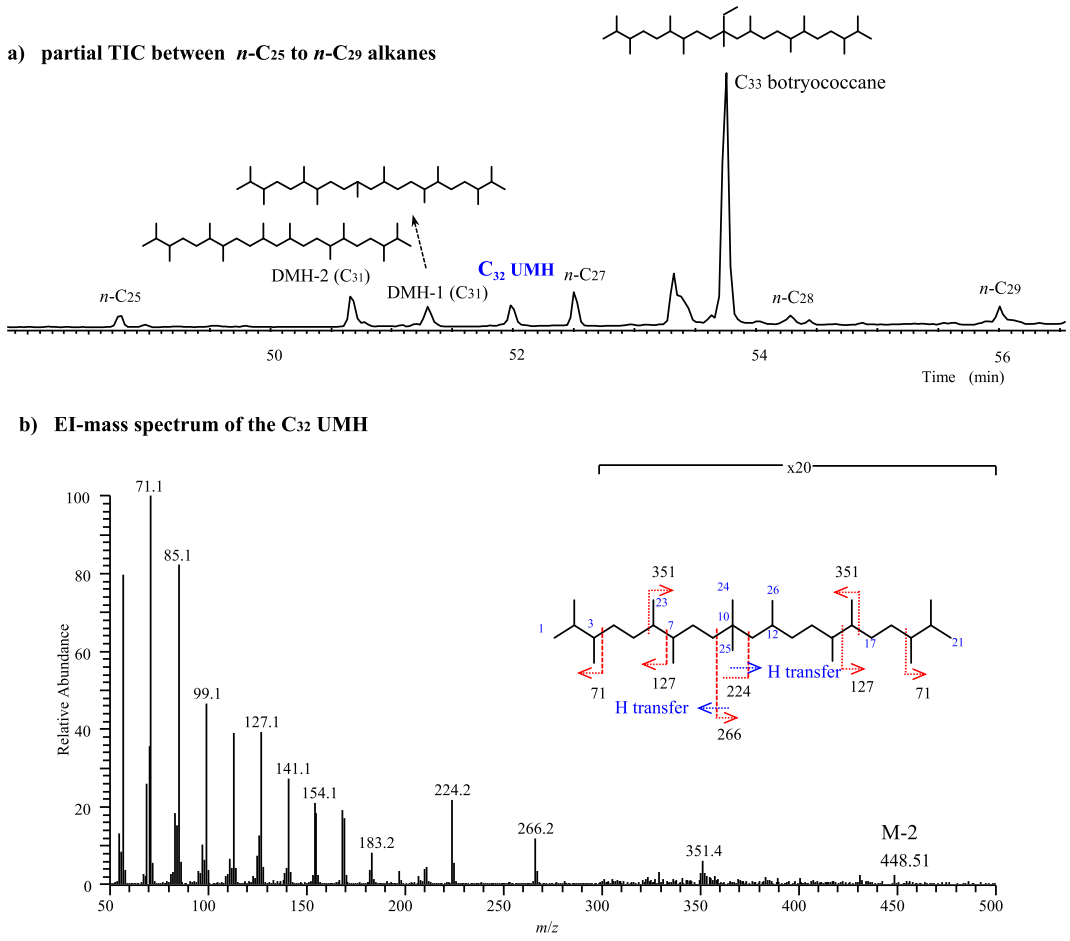

Fig. 1. Partial TIC (total ion current, a) of the saturated fraction of the extract from a sediment sample collected from Maoming Basin; EI-Mass spectrum of the C_{32} UMH (b).

A clear understanding of the pathway for the formation of their bio-precursors and how these bio-precursors are diagenetically stabilized is obviously of paramount importance for reliable geochemical applications of such biomarkers. Since a C_{33} botryococcan-24-one with the carbonyl group on the side chain was also isolated from the polar fraction of the sediment sample and proposed to be the oxygenated precursor of C_{33} botryococcanes (Liao et al., 2018a), we suspected that the oxygenated precursor(s) for the C_{32} botryococcane might also occur in the polar fraction. In this paper we report the isolation and structural elucidation of the C_{32} botryococcane and three oxygenated botryococcanoids by a combination of NMR, GC–CIMS and GC–EIMS techniques and discuss their genetic relationship in the context of our newly proposed cyclobutane cation-involving biosynthetic pathway (Liao et al., 2018a, 2018b) responsible for the formation of β-positioned methyl group in the botryococcanoid skeleton.

2. Material and methods

2.1. Isolation and purification

The C_{32} botryococcane and the oxygenated botryococcanes were extracted from the same Eocene sediment sample examined by Liao et al. (2018a, 2018b). The sample was collected from an oil shale outcrop in the Maoming Basin located in SW Guangdong Province, China, and transported back to the laboratory in a clean cloth bag. In the laboratory, the surface layer was carefully scraped off, leaving only the inner fresh part for organic matter extraction. After being powdered, organic matter was Soxhlet-extracted with CH_3OH/CH_2Cl_2 (1:9, v/v) for 72 h. The maltene fraction was obtained by centrifugally removing the asphaltene after precipitating the extractives in *n*-hexane. Saturated, aromatic and polar fractions were further separated from the maltene fraction by sequential elution with *n*-hexane (80 ml), *n*-hexane/dichloromethane (3:2, v/v, 50 ml) and methanol (30 ml), in a glass column (0.3 m × 1 cm i.d.) filled with activated silica (80–100 mesh)/aluminium oxide (4:1, v/v). The polar fraction was further sub-fractionated on a column (0.3 m × 1 cm i.d.) packed with silica (100–230 mesh), activated at 120 °C for 12 h, by eluting with CH_2Cl_2/*n*-hexane (1:3, v/v, 40 ml: subfraction N-1), CH_2Cl_2/*n*-hexane (1:2, v/v, 40 ml, subfraction N-2) and CH_2Cl_2/*n*-hexane (1:1, v/v, 40 ml: subfraction N-3). Throughout the whole procedure, care was taken to ensure no contamination was introduced to the samples.

The C_{32} botryococcane was eluted from the saturated hydrocarbon fraction and purified (2.0 mg) by preparative gas chromatography (PGC) (Özek and Demirci, 2012; Zuo et al., 2013) on an Agilent 7890 gas chromatograph interfaced to a Gerstel-preparative fraction collector (PFC), similar to that described by Eglinton et al. (1996). High purity helium (He) was used as carrier gas at a constant 3.0 ml/min flow rate. A DB-5 column (60 m × 0.53 mm × 1.5 μm film thickness) was used for separation. The column temperature was held at 80 °C for 2 min, then programmed to 300 °C at 30 °C/min, and held for 40 min. Using GC–MS and GC-FID analysis the purity was greater than 95% (Supplementary Fig. S1). The

purified target compounds were then subjected to gas chromatography-chemical ionisation mass spectrometry (GC–CIMS), and nuclear magnetic resonance (NMR) analysis for their structural assignment.

The polar fraction was subjected to GC–EIMS (gas chromatography–electron impact mass spectrometry) analysis using the same column and chromatographic conditions as described in Liao et al. (2018a). No preparative work was performed on the three oxygenated compounds.

2.2. Derivatisation

To support the identification of the alcohols in the sample, an aliquot of the subfraction N-3 of the polar fraction dissolved in 1 ml hexane was mixed with 1 ml BSTFA (N,O-*bis*(trimethylsilyl) trifluoroacetamide containing TMCS (trimethylchlorosilane) (99:1, v/v)). After 4 h at 40 °C and 12 h reaction at room temperature, the sample was then evaporated to dryness under a stream of N_2. The derivatised residue was then dissolved in hexane and analyzed by GC–EIMS and Q Exactive GC Orbitrap GC–MSMS. The underivatised sub-fraction N-3 was also analyzed via GC–EIMS using the same column and chromatographic conditions as that of the derivatised residue.

2.3. Instrumental analysis

GC–CIMS was performed on a Shimadzu QP2010 GC–MS equipped with a chemical ionisation source in the positive mode. Helium was employed as the carrier gas at a constant flow of 3 ml/min. The column temperature was programmed from 80 °C (held for 2 min) to 295 °C (held for 25 min) at a rate of 6 °C/min. Methane was used as the reagent gas. ^{1}H and ^{13}C Nuclear Magnetic Resonance (NMR) spectral analyses were conducted on a Bruker AVANCE III 600 MHz NMR spectrometer (operating at 600.19 MHz for ^{1}H NMR and 150.92 MHz for ^{13}C NMR). Spectra were recorded in $CDCl_3$ solutions, with TMS as internal standard. ^{1}H NMR chemical shifts were referenced relative to the residual proton signal (7.26 ppm) while ^{13}C NMR chemical shifts were referenced to the central line of the ^{13}C multiplet (77.0 ppm) of $CDCl_3$. A combination of ^{13}C spectral and distortionless enhanced polarization transfer (DEPT) spectra (DEPT 90° and 135°) were performed to determine the multiplicity of each ^{13}C nucleus. 2D NMR experiments ^{1}H–^{1}H correlation spectroscopy (COSY), ^{1}H–^{13}C heteronuclear single quantum coherence (HSQC), and ^{1}H–^{13}C heteronuclear multiple bond correlation (HMBC) were used to assign the individual resonances.

GC–EIMS analysis of compounds was performed using a Trace Ultra GC interfaced with a Thermo DSQ-II mass spectrometer operating at 70 eV with a mass range of *m/z* 50–600. A HP-5 column (30 m × 0.25 mm × 0.25 μm film thickness) was used for separation. The column temperature for analysing the polar fraction was programmed from 80 °C (held for 2 min) to 295 °C (held for 35 min) at a rate of 3 °C/min (Fig. 4a). The oven temperature for GC separation of the sub-fraction N-3 before and after TMS-derivatisation was programmed from 80 °C (held for 2 min) to 295 °C (held for 20 min) at a rate of 4 °C/min (Fig. 5a). High purity He was used as carrier gas at a flowrate of 1.2 ml/min.

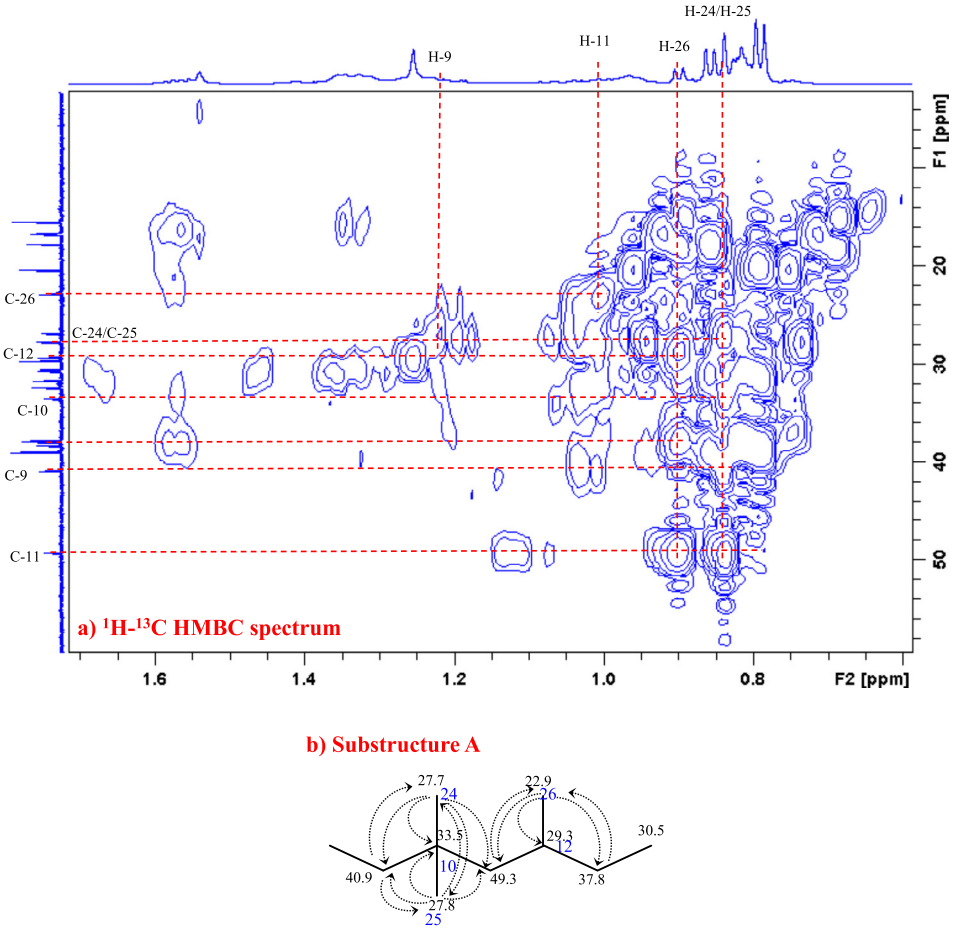

Fig. 2. ^{1}H–^{13}C HMBC spectrum (a) and the assignment (b) for the substructure **A** of the new C_{32} UMH in this study.

3. Results and discussion

3.1. Identifying the C_{32} botryococcane (C_{32} UMH)

In the TIC of the saturated fraction examined by Liao et al. (2018a, 2018b), a prominent peak was observed to elute between the two C_{31} DMHs and C_{33} botryococcane (Fig. 1a). To ascertain its carbon number and structure, we purified this compound by preparative gas chromatography and structurally characterised it by GC–CIMS and 2D NMR.

GC–CIMS analysis gave a molecular adduct ion ($[M + CH_5]^+$) at m/z 467.5 (Supplementary Fig. S2; see also Supplementary Fig. S1 for the TIC of the purified compound) for the peak, in agreement with the 450 Da molecular weight (MW) determined for $C_{32}H_{66}$.

The ^{13}C NMR spectrum (Supplementary Figs. S3 and S5) contained 28 resonances (interfering peak δc 29.7 ppm from long-chain alkanes excluded) which can be ascribed to 1C, 9 CH, 9 CH_2 and 13 CH_3 according to the DEPT experiments (note that CH: δc 39.0, 37.9 ppm, CH_3: δc 20.4, 15.5 ppm are overlapping resonances) (Supplementary Fig. S5). The multiplicity of ^{13}C nucleus was obviously in accordance with the result of GC–CIMS analysis.

To assign the resonances to the carbons in the skeleton, and in particular, in the substructure **A** (Fig. 2), we looked at the ^1H–^{13}C HMBC correlations (see also NMR data for ^{13}C and ^1H in Table 1). The H-24 and H-25 were singlet (Fig. 2a), and C-24 and C-25 were both directly connected to the quaternary carbon C-10. The correlations (Fig. 2) from H-24/25 to C-9 and C-11 indicated the connections between C-9/C-10 and C-10/C-11. Such connections are also supported by the correlations (Fig. 2a) between H-9 and C-24, H-24 and C-25, H-25 and C-24, H-24/25 and C-10. As C-11, C-12, C-13 were correlated with H-26 (Fig. 2a), it is reasonable to assign the C-26 methyl to C-12, and connections between C-11/C-12 and C-12/C-13 (Fig. 2b).

Using the ^1H–^{13}C HMBC and ^1H–^1H COSY spectra (Supplementary Fig. S7), the resonances were also assigned to the carbons in substructure **B** and **B́** (Fig. 3a, Table 1). The assignment is supported by the fact that **B** and **B́** are the same substructures in the decamethylhenicosane-1 (DMH-1, Fig. 3b) identified by us (Liao et al., 2018b) from the same Maoming sediments and in the sacredicene (Fig. 3c) identified by Huang et al. (1995) from lake sediment, and that the position-specific differences of the chemical shift δc values for all carbons between the substructures **B** and **B́** and their equivalent substructures in DMH-1 and sacredicene were less than 0.2 ppm. Since the ^1H–^{13}C HMBC correlation (Fig. 3a) between H-31 and C-14 indicated a C-14/C15 connection while COSY correlation between H-14 and H-13 showed a C-13/C-14 connection, substructure **B́** must be on the right side of the substructure **A**. This is further supported by the fact that ^1H–^{13}C HMBC correlation (Fig. 3a) from H-9 to C-8 showed a C-8/C-9 connection (implying a left-side-positioned substructure **B**). Since the new C_{32} alkane identified here has 21 carbons in the backbone and 11 methyl groups attached to the backbone, it is thus named as 2,3,6,7,10,10,12,15,16,19,20-undecamethylhenicosane (C_{32} UMH).

The NMR-based structural assignment for C_{32} UMH is also supported by the EI-mass spectrum (Fig. 1b): The characteristic ions at m/z 224 and 266 are the result of cleavages around the sole quaternary carbon (C-10) with hydrogen migration. The low intensity ion at m/z 448 is interpreted as a (double) deprotonated molecular ion m/z 450 $[M-2H]^{+\cdot}$. The base ion at m/z 71 (C_5H_{11}) is interpreted to be the result of the cleavage of C-3/C-4 and C-18/C-19 bonds. The ion at m/z 351 is the result of the cleavage of C-5/C-6 and C-16/C-17 bonds.

To further confirm the new skeleton inferred from NMR analysis, Lindeman and Adams modelled (Lindeman and Adams, 1971) δ_C values were compared with the measured δ_C values for the proposed new skeleton (Fig. 3a,d). As shown in Fig. 3a,d, the position-

Table 1
^1H (600 MHz) and ^{13}C (150 MHz) NMR data of the C_{32} UMH recorded in $CDCl_3$.

Position	^1H, δ (ppm), Multiplicity (J in Hz)	^{13}C, δ (ppm), multiplicity	DEPT	HMBC ($^1H \rightarrow ^{13}C$)	^1H–^1H COSY cross peaks
1	0.790, d (6.72)	17.8, q	CH_3	22	1.566
2	1.566, overlap	31.7, d	CH	1, 22, 29	0.790, 0.858, 1.235
3	1.235, overlap	39.0, d	CH	1, 22	0.790, 1.566
4	1.353, overlap; 0.962, overlap	30.6, t	CH_2		0.965
5	1.353, overlap; 0.965, overlap	32.4, t	CH_2		1.353
6	1.321, overlap	37.9, d	CH	30	0.824
7	1.321, overlap	38.0, d	CH	23	0.812
8	1.258, overlap; 0.957, overlap	26.9, t	CH_2	9	
9	1.233, overlap; 1.063, m	40.9, t	CH_2	11, 24, 25	
10		33.5, s	C	24, 25	
11	1.196, m; 1.019, m	49.3, t	CH_2	24, 25, 26	1.407
12	1.407, m	29.3, d	CH	26	0.899, 1.019, 1.196
13	1.321, overlap; 1.002, m	37.8, t	CH_2	26	0.962
14	1.324, overlap; 0.962, overlap	30.5, t	CH_2	31	1.321
15	1.321, overlap	38.3, d	CH	27	0.812
16	1.321, overlap	37.9, d	CH	31	0.812
17	1.353, overlap; 0.965, overlap	32.4, t	CH_2		1.353
18	1.353, overlap; 0.962, overlap	30.8, t	CH_2		0.962
19	1.235, overlap	39.0, d	CH	21, 28	0.790, 1.566
20	1.566, m	31.7, d	CH	21, 28, 32	0.790, 0.858, 1.235
21	0.790, d(6.72)	17.8, q	CH_3	28	1.566
22	0.858, d(6.96)	20.4, q	CH_3	1	1.566
23	0.824, overlap	16.7, q	CH_3		1.321
24	0.838, s	27.7, q	CH_3	25	
25	0.838, s	27.8, q	CH_3	24	
26	0.899, d(6.48)	22.9, q	CH_3	13	1.407
27	0.819, overlap	16.7, q	CH_3		1.321
28	0.858, d(6.96)	20.4, q	CH_3	21	1.566
29	0.790, d(6.72)	15.5, q	CH_3		1.235
30	0.812, overlap	16.8, q	CH_3		1.321
31	0.812, overlap	16.8, q	CH_3		1.321
32	0.790, d(6.72)	15.5, q	CH_3		1.235

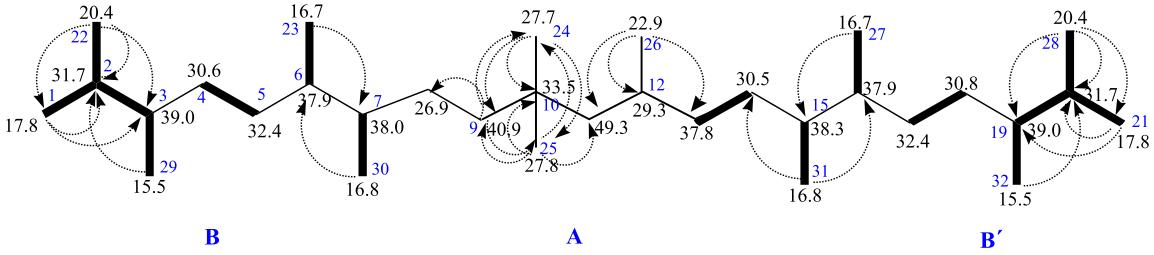

a) ^{1}H-^{13}C HMBC correlations and ^{1}H-^{1}H COSY bonds for the assignment of the UMH in this study

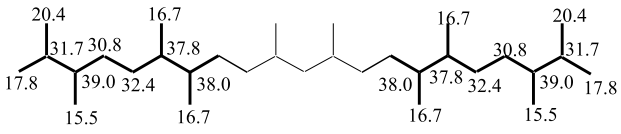

b) DMH-1 from Liao et al. (2018b)

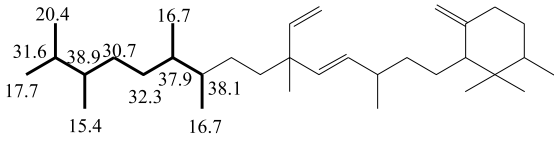

c) sacredicene from Huang et al. (1995)

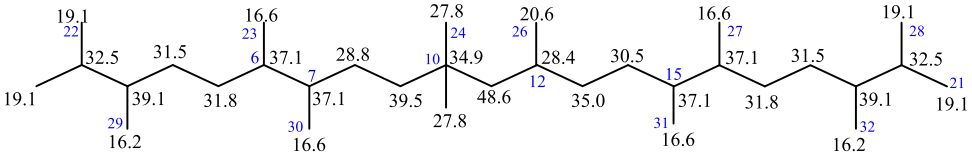

d) calculated δ_C values of the newly identified UMH by Lindeman and Adams computing (1971)

Fig. 3. Key correlations for structural assignment for the new skeleton and its δ_C value assignment. Key ^{1}H–^{1}H COSY (bond bolds) and HMBC correlations (^{1}H→^{13}C) of C_{32} UMH (a); measured δ_C values for the substructures **B** and **B′** of UMH (a), DMH-1 from Liao et al. (2018b) (b), and Huang et al. (1995) (c); modelled δ_C values for the new skeleton of UMH identified in this study (d).

specific discrepancies for the majority of the carbons were minimal, and the maximum discrepancy is less than 1.5 ppm. This confirms the robustness of the identification.

3.2. Identifications of C_{32} undecamethylhenicosanal (C_{32} UMH-al) and C_{31} decamethylhenicosanols (C_{31} DMH-ols)

The peak eluting at 70.7 min (marked with solid red inversed triangle; see Fig. 4a for the TIC of the polar fraction) displayed two prominent ions in its mass spectrum: *m/z* 240 and 282 (Fig. 4c, note that *m/z* 281 is largely from a slightly co-eluting peak), both 14 Da lower than the characteristic ions of *m/z* 254 and 296 for the C_{33} botryococcan-24-one identified in the same sample (Fig. 4b; Liao et al., 2018a). This 14 Da difference was also evident in the molecular ion (*m/z* 464) when compared with that of C_{33} botryococcan-24-one (*m/z* 478). These suggest that this peak may be an oxygenated botryococcane with a skeleton similar to that of the C_{33} botryococcan-24-one and could therefore be reasonably assigned a formula of $C_{32}H_{64}O$. As two additional characteristic ions at *m/z* 435 [M^+−29] and *m/z* 449 [M^+−15] can be successfully explained by the loss of an aldehyde group (Fig. 4c) and a methyl group connected to the sole quaternary carbon C-10 respectively (Fig. 4c), a C_{32} aldehyde (C_{32} botryococcanal, C_{32}-UMH-al) can be speculated. Indeed, ions at *m/z* 240 and 282 could also be attributed to a McLafferty rearrangement (γ-H migration and β cleavage) as shown in Fig. 4c, which is also responsible for the generation of the ions of *m/z* 254 and 296 for the C_{33} botryococcan-24-one (Fig. 4b, Kingston et al., 1974; Liao et al., 2018a).

The mass spectra (Fig. 4d; only one spectrum is shown here as the two mass spectra are essentially the same) of the two peaks (marked with hollow red inversed triangles, Fig. 4a) eluted before the C_{32} UMH-al were dominated by ions *m/z* 227 and 269. Since these two ions are both 13 Da lower than the two characteristic ions 240 and 282 in the C_{32} UMH-al spectrum, and that ions *m/z* 434 and *m/z* 437 can be easily explained by the loss of a neutral water molecule and a methyl group (connected to the sole quaternary C-10) respectively from a DMH alcohol with one carbon short (than the C_{32} UMH-al, Fig. 4d), it is reasonable to assign these two peaks to C_{31} DMH-ol. The two characteristic ions, *m/z* 227 and 269 can be easily explained by α-cleavages around the quaternary carbon (Fig. 4d). Since the mass spectra of these two C_{31} DMH-ols are essentially the same, it is reasonable to assume they are epimers.

To further ascertain the structural assignment of the two alcohols, we trimethylsilylated the sub-fraction N-3 of the polar fraction which contained the two alcohols. The mass spectra of the two trimethylsilylated peaks (eluted at 47.7 and 47.8 min respectively; Fig. 5a, marked with hollow red inversed triangles) indeed showed two dominant ions at *m/z* 299 and 341 (Fig. 5b and c), corresponding to the two observed ions *m/z* 227 and 269 in the underivatized peaks with an additional TMS group. The intense ion at *m/z* 509 can then be easily explained by the loss of a methyl group from the ionized trimethylsilyl group. The identifications of the two TMS derivatives were also supported by the close match of the accurate masses of the fragments obtained on a Q Exactive Orbitrap MS (see Supplementary Figs. S8 and S9) with that of theoretical calculations: the accurate masses of fragments ions *m/z* 299.2764 $[C_{18}H_{39}OSi]^+$, 341.3232 $[C_{21}H_{45}OSi]^+$ and 509.5112 $[C_{30}H_{60}OSi]^+$ ($[M-CH_3]^+$) of DMH-OTMS-1 (see Supplementary Fig. S8) and 299.2762, 341.3231 and 509.5113 of DMH-OTMS-2 (see Supplementary Fig. S9) were in excellent agreement with the calculated masses of 299.2769, 341.3239, and 509.5117 respectively.

3.3. Bacterial formation of the C_{31}–C_{33} botryococcanes and their oxygenated homologues

Based on the identification of co-occurring C_{33} botryococcane (**17**, Fig. 6), C_{33} botryococcanone (**10**) and two C_{31} botryococcanes

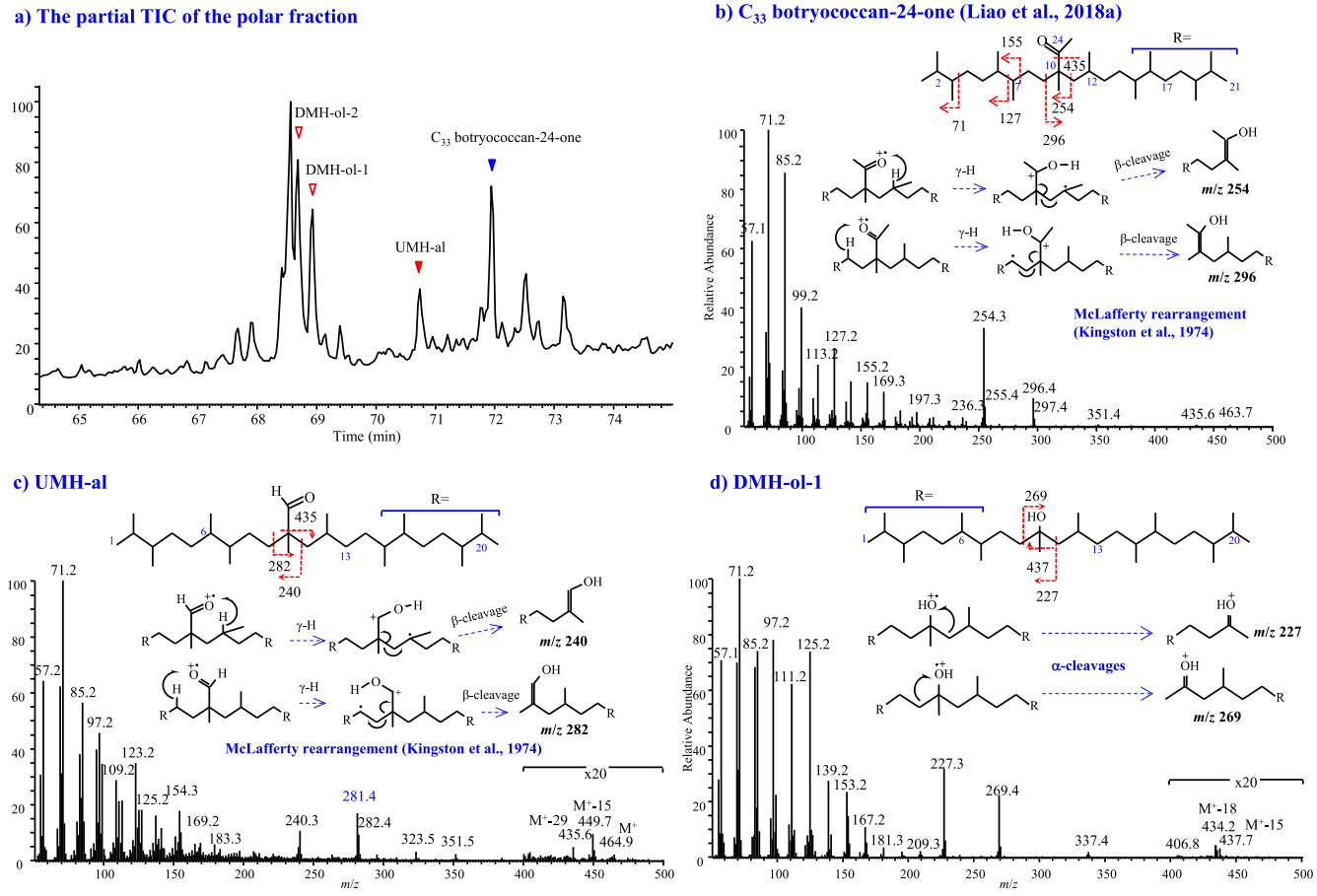

Fig. 4. The partial TIC (total ion current) of the polar fraction of the sample showing the elution order of the three oxygenated botryococcanoids (a) and the mass spectra for the C_{33} botryococcanone (b, see also Liao et al., 2018a), the C_{32} UMH-aldehyde (c) and two C_{31} DMH-alcohols (d).

(**21** and **22**) (Liao et al., 2018a, 2018b), we recently proposed that these alkanes and ketone are the diagenetically stabilized C_{33} botryococcene (**2**) formed as a result of an unusual in vivo c1′-2-3-2′ condensation (cyclobutanation) of two FPPs (farnesyl diphosphates, **1**) followed by a *retro*-Prins (with one carbon loss) and subsequent tetramethylation (with four carbon gain). The oxidation of the C=C double bond at the ethenyl group (CH_2=CH) of C_{33} botryococcene (**2**) for the formation of the C_{33} alkenone (**7**) and a hypothetical C_{32} botryococcenic acid (**9**) (a hypothetical intermediate for the formation of the two C_{31} botryococcanes) were suspected to be the result of photo-mediated oxidation in oxic shallow water in Liao et al. (2018b).

Although the formation of the stabilized C_{33} botryococcene (**2**) can be well explained by the unusual cyclobutanation (Liao et al., 2018a), the proposed photo-mediated oxidation of the C=C double bond at the ethenyl group (CH_2=CH, at C24-25) of C_{33} botryococcene (**2**) might need further examination. Abiotic degradation (photo-oxidation and autoxidation) of highly branched isoprenoid (HBI) alkenes (Rontani et al., 2011, 2014, 2018, 2019) with similar multi-branched structure to botryococcanoids has been shown to act preferentially (Rontani et al., 2011, 2014, 2018, 2019) on internal (or trisubstituted) double bonds rather than on terminal ones. HBI alkenes with at least one trisubstituted double bond photodegraded at similar or higher rates than some other lipids (e.g., vitamin E) known to be very reactive towards singlet oxygen $^1O_2$. On the other hand, photo- and autoxidation degradation rates of mono-unsaturated C_{25} HBI alkene (**23**) with the double bond on the terminal position (i.e. at C23-24) and di-unsaturated C_{25} HBI alkene (**24**) with the double bonds on the terminal positions (i.e. at C6-17 and C23-24) (see Appendix A for structures of **23** and **24**) previously studied in vitro (Rontani et al., 2011, 2014, 2018) were very low, indicating that the terminal double bonds of HBI alkenes would be largely unaffected by abiotic oxidation within the water column. Theoretically, the C–H bond energy for allylic hydrogens is lower for internal double bonds than it is for terminal double bonds (77 kcal/mol vs 85 kcal/mol; Schaich, 2005), thus making internal double bonds more reactive. Calculation of the degradation rates of $^1O_2$ with various double bonds also indicates the greater reactivity of the internal double bond (trisubstituted double bond: 7.2×10^5 $M^{-1}S^{-1}$) than the terminal one (4.0×10^3 $M^{-1}S^{-1}$) (Hurst et al., 1985), so that for the C_{33} botryococcene (**2**), the photo-mediation or autoxidation would also preferentially act on the trisubstituted double bond (at C11-12) rather than the terminal ones (i.e. at C24-25 and C3-30) (see Appendix A for carbon numbering of **2**). Based on the C_{31}–C_{32} botryococcanes and their oxygenated homologues identified here, the oxidation of the double bond of C_{33} botryococcene (**2**) is presumed to have acted on the terminal double bond (at C24-25) while the trisubstituted double bond (at C11-12) was unaffected. Thus, the degradation of the C_{33} botryococcene (**2**) might not be due to photo-mediated oxidation or autoxidation.

If the abiotic degradation is unlikely, biotic degradation of the C_{33} botryococcene (**2**) may be occurring. This has a parallel, as previously demonstrated by Rontani et al. (2018), in that mono-unsaturated C_{25} HBI alkene (**23**) (also isoprenoid alkenes) with a terminal double bond (at C23-24) can be rapidly biodegraded by sedimentary bacteria under aerobic or anaerobic conditions to produce 3,9,13-trimethyl-6-(1,5-dimethylhexyl)-tetradecan-1,2-diol

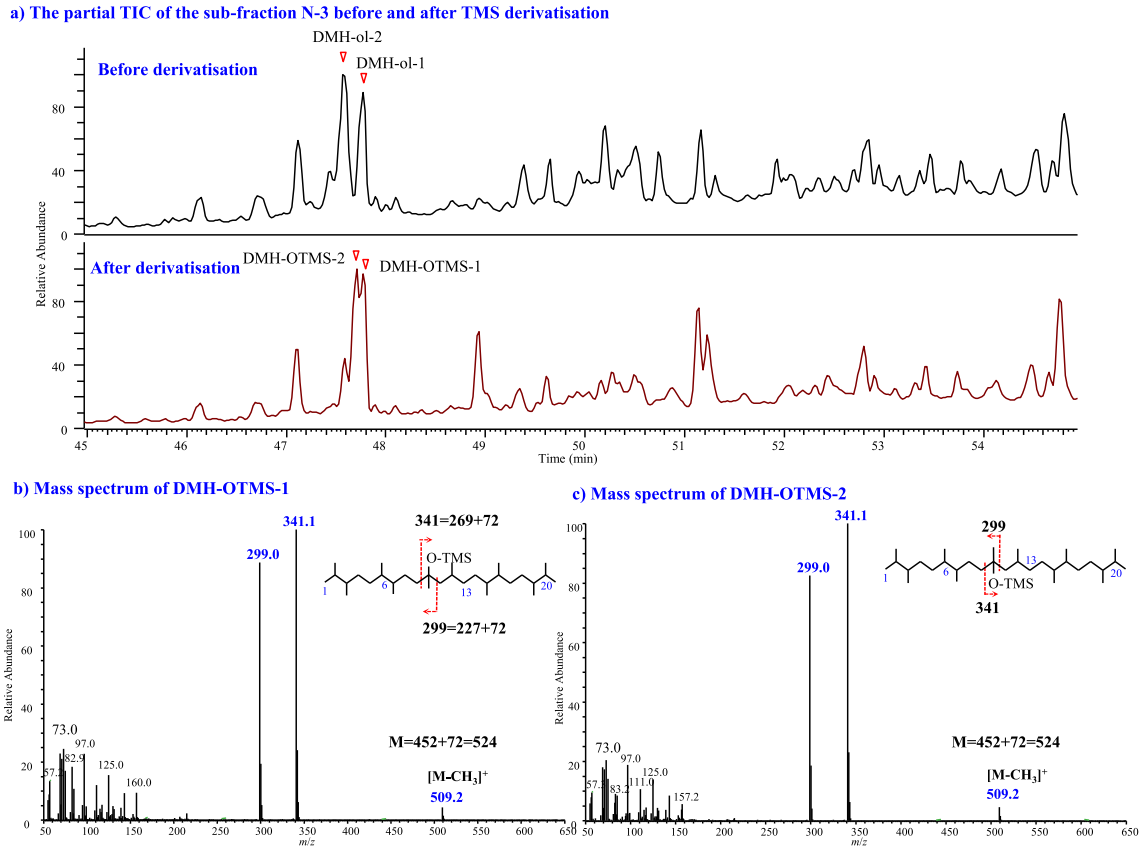

Fig. 5. The partial TIC of the sub-fraction of N-3 before and after TMS derivatization showing the elution order of the speculated two DMH-ols, DMH-OTMS (a) and the mass spectra for the DMH-OTMS-1 (b) and the DMH-OTMS-2 (c).

(**25**) and 2,8,12-trimethyl-5-(1,5-dimethylhexyl)-tridecanoic acid) (**26**) (see Appendix A for structures of **25** and **26**). The degradation of the terminal double bond (at C24-25) of the C_{33} botryococcene (**2**) might thus be mediated by bacteria, therefore a bacterially mediated degradation pathway from C_{33} botryococcene (**2**) to C_{31}–C_{32} botryococcanes and their oxygenated derivatives could be proposed.

Bacterial degradation of the double bond in C_{33} botryococcene (**2**) can produce C_{33} botryococcenol (**4**) and C_{33} botryococcene diol (**5**) via the corresponding C_{33} botryococcene epoxide **3** (Soltani et al., 2004; Rontani et al., 2018) (Fig. 6) based on microbial glutathione transferases and microbial epoxide hydrolase, respectively (Swaving and de Bont, 1998). Previously, it was demonstrated that various pristenes and phytenes can be rapidly biodegraded by sedimentary bacteria under anaerobic conditions, mainly by hydration reactions (Rontani et al., 2013). In the case of C_{33} botryococcene (**2**), anaerobic addition of water to the C24-25 double bond also results in the direct formation of C_{33} botryococcenol (**4**) (Fig. 6), which subsequently oxidizes to a hypothetical ketone C_{33} botryococcenone (**7**). Hydrogenation in sediment saturates **7**, leading to firstly the C_{33} botryococcanone (**10**) and subsequently to a C_{33} botryococcanol (**13**). On being dehydrated and hydrogenated, **13** can be stabilized as the C_{33} botryococcane (**17**) (Fig. 6).

Since a C_{32} botryococcanal (**11**) was identified here from the same sample, we further hypothesize that a C_{32} botryococcenal (**8**) must have existed. This hypothesis is supported by occurrence of steranes and hopanes (hydrogenated products of corresponding sterenes and hopenes during early digenesis) in many immature samples (e.g., Brassell et al., 1986; Chen et al., 1994; Schouten et al., 1997), which indicates that alkenes can be easily hydrogenated geochemically to alkanes during digenesis. Under such a hypothesis, the C_{32} alkane (**18**, C_{32} UMH) identified here could be the stabilized product of this alkanal (**11**) via an inferable C_{32} alcohol (**14**) (Fig. 6). This hypothesis also fills the gap between the alkene (**2**) and alkenoic acid (**9**) as implied by Liao et al. (2018b). Previously, Rontani et al. (2018) proposed that a diol oxidized from mono-unsaturated C_{25} HBI alkene (**23**) might be cleaved to form 2,8,12-trimethyl-5-(1,5-dimethylhexyl)-tridecanal (**27**) (see Appendix A for structure of **27**) with the loss of a $–CH_2O$. In the case of the C_{33} botryococcene diol (**5**), C-C cleavage might lead to the loss of a $–CH_2O$ group, resulting in the formation of the C_{32} botryococcenal (**8**) (Fig. 6).

Bacterial oxidation of the hydroxy in the C_{33} botryococcene diol (**5**) can produce a botryococcene hydroxy acid (**6**), and subsequently the C_{32} botryococcenoic acid (**9**) by oxidative decarboxylation (Fig. 6). Oxidation of the C_{32} botryococcenal (**8**) could also afford the C_{32} botryococcenoic acid (**9**). Oxidation of the ethylene group of the C_{33} botryococcene (**2**) may also directly afford **8** and subsequently **9**. Decarboxylation of **9** with a double bond positioned β- to the sole carboxyl group affords a C_{31} botryococcene (**12**) with the double bond migrating to position C10-11 (Fig. 6) as described by Bigley and Clarke (1982) for β-unsaturated acids. The C_{31} epimeric DMH-ols (**19** and **20**) identified here might be geochemically hydrogenated from two epimeric C_{31} botryococcenols (**15** and **16**), which can be produced by *syn*- or *anti*-hydration (Jin and Hanefeld, 2011; Resch and Hanefeld, 2015) of the migrated double bond (C10-11) in **12** (see Appendix A for carbon numbering of **12**). It is interesting that the two C_{31} epimeric botryococcenols (**15** and **16**) can be interconverted via an epimerase (Jin and Hanefeld, 2011). The two identified C_{31} epimeric DMHs (**21** and **22**) in Liao et al. (2018b) could be the stabilized products of

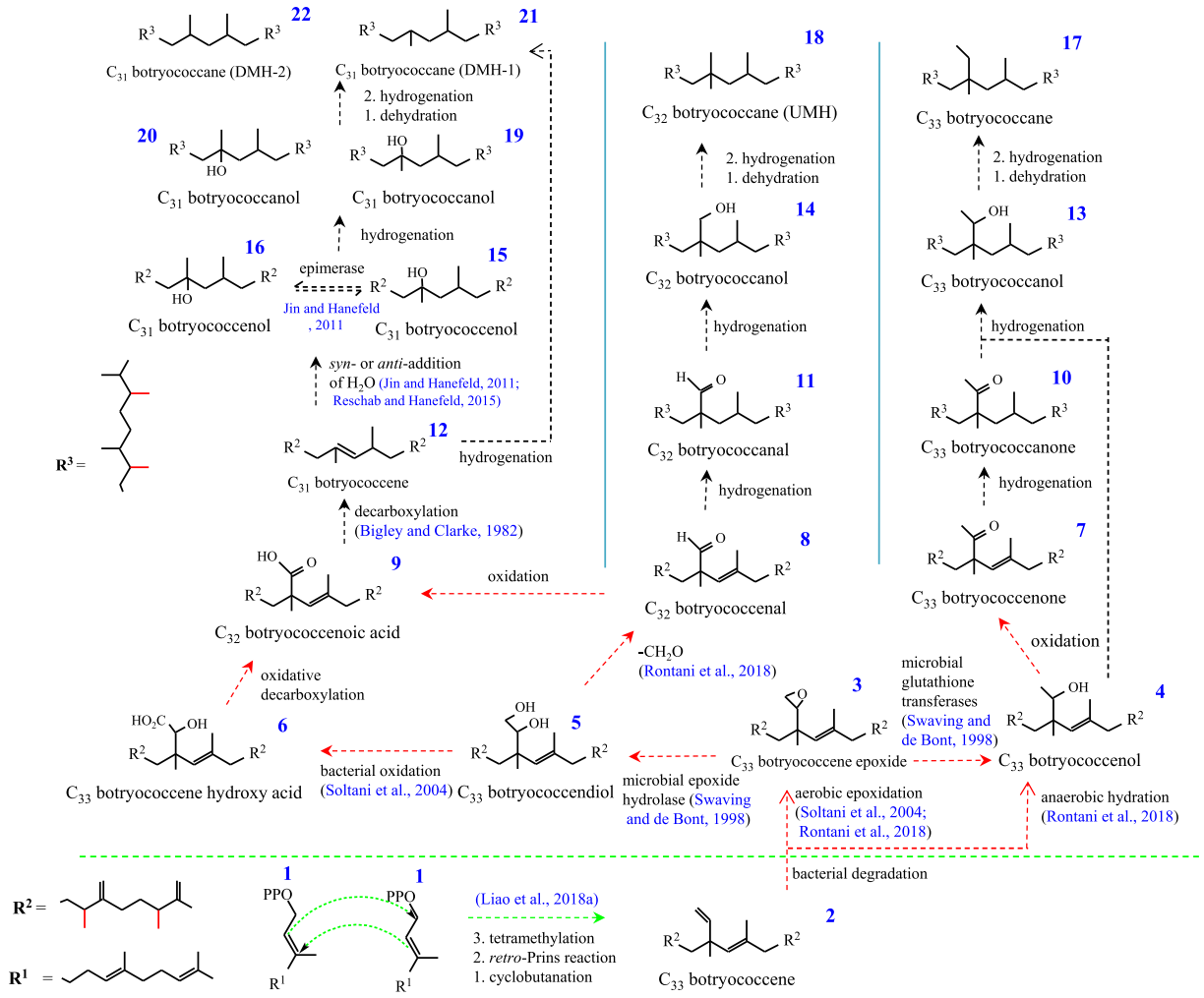

Fig. 6. The biogeochemical pathway proposed for the formation of the C_{31}–C_{33} botryococcanoids (alkanes, alkanals, alkanols) identified here and previously by Liao et al. (2018a, b). The green, red and black dashed arrows are for the reactions associated with biological, bacterial and diagenetic processes, respectively. (For interpretation of the references to colour in this figure legend, the reader is referred to the web version of this article.)

the two C_{31} epimeric DMH-ols (Fig. 6). Geochemically, hydrogenation of **12** might also produce the two C_{31} epimeric DMHs (**21** and **22**), but might show preference for the configuration of the products. Geochemical hydrogenation of one double bond would produce two configurations, and more double bonds, more configurations. There would be a big difference in abundance of these produced configurations. Five double bonds exist in **12**, however, only two configurations, with nearly the same abundance, were observed. Thus, the two C_{31} epimeric alcohols (**19** and **20**) may be the major contributors to the formation of the two C_{31} epimeric alkanes (**21** and **22**). Previously, decarboxylation of the C_{32} botryococcenoic acid (**9**) for the production of the two epimeric C_{31} alcohols (**19** and **20**) (Liao et al., 2018b) was proposed via a putative C_{31} tertiary carbocation but this was inconsistent with opinions expressed by Brown (1951) and not considered further.

The formation of the C_{31} and C_{32} botryococcanes and their oxygenated homologues identified in Liao et al. (2018b) and in this paper begins with bacterial degradation of the terminal double bond positioned at the ethenyl group connected to the sole quaternary carbon of the C_{33} botryococcene (**2**), followed by further bacterial degradation as outlined in Fig. 6. The fact that these oxidized ethenyl groups of the botryococcene derivatives have not been previously reported may be indicative of the presence of unique bacterial flora in the Maoming oil shale. This will require further research.

4. Conclusions

Based on our recent identifications of a C_{33} botryococcane, a C_{33} botryococcanone and two C_{31} botryococcanes, we propose that their common bio-precursor is a C_{33} botryococcene with a unique methyl group β-positioned to the sole quaternary carbon in the skeleton. Such a precursor is formed by an unusual condensation of two FPPs involving a cyclobutanation (rather than the currently accepted cyclopropane) intermediate, a *retro*-Prins reaction and a subsequent tetramethylation. Abiotic degradation (photo-mediated or autoxidation) preferentially acts on the internal double bond rather than the terminal ones. Sedimentary bacteria, however, could preferentially biodegrade the terminal double bond leaving the trisubstituted double bond (at C11-12) unaffected. We now propose that there was bacterially mediated oxidation of the ethenyl group connected to the sole quaternary carbon in the C_{33} botryococcene yielding the C_{31} and C_{33} alkanes and C_{33} alkanone and the C_{32} UMH identified here. Nevertheless, the putative presence of aldehyde, alcohol and acidic moieties along the pathways for the formation of the C_{31}–C_{33} botryococcanes means that there is a gap in the geochemical pathway. With the identification of the saturated C_{32} UMH-aldehyde and two C_{31} epimeric DMH-alcohols, we propose a specific bacterial-mediated degradation pathway from C_{33} botryococcene to C_{31}–C_{33} botryococcanes and their oxygenated derivatives. The absence of the ethenyl

group-oxidized (that connected to the sole quaternary carbon) botryococcene derivatives in other samples implies some unique bacterial flora may be responsible for the formation of the C_{31}–C_{33} botryococcanes and their oxygenated homologues in the Maoming sediments. Further research on the proposed specific bacterial mediated pathway is needed.

Declaration of Competing Interest

The authors declare that they have no known competing financial interests or personal relationships that could have appeared to influence the work reported in this paper.

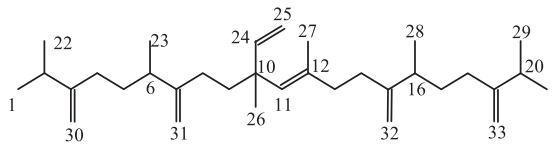

2 C_{33} botryococcene

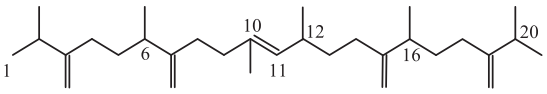

12 C_{31} botryococcene

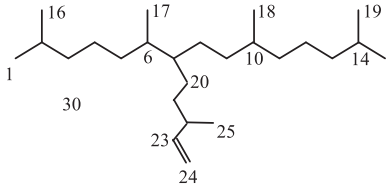

23 monounsaturated C_{25} HBI alkene

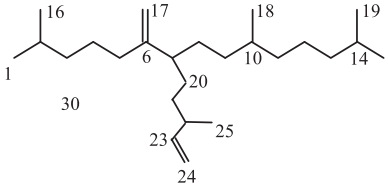

24 di-unsaturated C_{25} HBI alkene

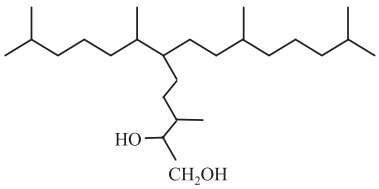

25 3,9,13-trimethyl-6-(1,5-dimethylhexyl) -tetradecan-1,2-diol

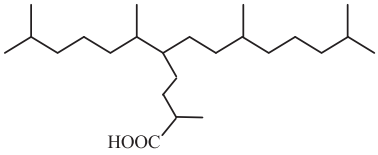

26 2,8,12-trimethyl-5-(1,5-dimethylhexyl) -tridecanoic acid

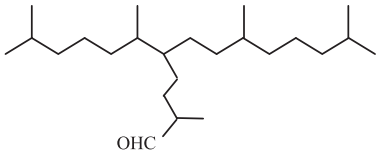

27 2,8,12-trimethyl-5-(1,5-dimethylhexyl) -tridecanal

Acknowledgements

The authors thank Drs. Y.K. Tian, and W.B. Zhang for their technical help with GC–MS and pGC instrumentation. HL acknowledges the financial support from the Strategic Priority Research Program of the Chinese Academy of Sciences (XDA14010102), the National Key R&D Program of China (2017YFC0603102), the GIG-135 Shale Gas Project, China (135TP201602), National Major Equipment Grants [2017ZX05008-002-030], Project SKLOG2016-A02, SKLOG2016-A08 and Chinese NSF grants (41673066, 41673045, and 41973069); YZ acknowledges the support of a Chinese NSF grant (41773032) and a Shaanxi Department of Education grant (17JS013); JL acknowledges the support of a Chinese NSF grant (41903064) and a Chinese Postdoctoral Science Foundation (2019M663131). Prof C.H. Hocart is gratefully acknowledged for improving the English in the manuscript. We thank the reviewers for their helpful comments. This is contribution No. IS-2791 from GIGCAS and #10 from the Isotopomics in Chemical Biology group.

Appendix A

Appendix B. Supplementary data

Supplementary data to this article can be found online at https://doi.org/10.1016/j.orggeochem.2020.103974.

Associate Editor—**Sylvie Derenne**

References

Bigley, D.B., Clarke, M.J., 1982. Studies in decarboxylation. Part 14. The gas-phase decarboxylation of but-3-enoic acid and the intermediacy of isocrotonic (*cis*-but-2-enoic) acid in its isomerisation to crotonic (*trans*-but-2-enoic) acid. Journal of the Chemical Society, Perkin Transactions II, 1–6.

Brassell, S.C., Eglinton, G., Fu, J.M., 1986. Biological marker compounds as indicators of the deposition history of the Maoming oil shale. Organic Geochemistry 10, 927–941.

Brown, B.R., 1951. The mechanism of thermal decarboxylation. Quarterly Reviews 5, 131–146.

Chen, Z.L., Zhou, G.J., Alexander, R., 1994. A biomarker study of immature crude oils from the Shengli oilfield, People's Republic of China. Chemical Geology 113, 117–132.

Eglinton, T.I., Aluwihare, L.I., Bauer, J.E., Druffel, E.R.M., McNichol, A.P., 1996. Gas chromatographic isolation of individual compounds from complex matrices for radiocarbon dating. Analytical Chemistry 68, 904–912.

Guy-Ohlson, D., 1992. *Botryococcus* as an aid in the interpretation of palaeoenvironment and depositional processes. Review of Palaeobotany and Palynology 71, 1–15.

Huang, Y., Murray, M., Eglinton, G., Metzger, P., 1995. Sacredicene, a novel monocyclic C_{33} hydrocarbon from sediment of Sacred Lake, a tropical freshwater lake, Mount Kenya. Tetrahedron Letters 36, 5973–5976.

Hurst, J.R., Wilson, S.L., Schuster, G.B., 1985. The ene reaction of singlet oxygen: kinetic and product evidence in support of a perepoxide intermediate. Tetrahedron 41, 2191–2197.

Jin, J., Hanefeld, U., 2011. The selective addition of water to C=C bonds; enzymes are the best chemists. Chemical Communications 47, 2502–2510.

Kingston, D.G.I., Bursey, J.T., Bursey, M.M., 1974. Intramolecular hydrogen transfer in mass spectra. II. McLafferty rearrangement and related reactions. Chemical Reviews 74, 215–242.

Liao, J., Lu, H., Feng, Q., Zhou, Y.P., Shi, Q., Peng, P.A., Sheng, G.Y., 2018a. Identification of a novel C_{33} botryococcane and C_{33} botryococcanone in the Maoming Basin, China. Organic Geochemistry 124, 103–111.

Liao, J., Lu, H., Feng, Q., Zhou, Y.P., Shi, Q., Peng, P.A., Sheng, G.Y., 2018b. Two novel decamethyl henicosanes ($C_{31}H_{64}$) identified in a Maoming Basin shale, China. Organic Geochemistry 125, 212–219.

Lindeman, L.P., Adams, J.Q., 1971. Carbon-13 nuclear magnetic resonance spectrometry. Chemical shifts for the paraffins through C_9. Analytical Chemistry 43, 1245–1252.

Maxwell, J.R., Douglas, A.G., Eglinton, G., McCormick, A., 1968. The Botryococcenes–hydrocarbons of novel structure from the alga *Botryococcus braunii*, Kützing. Phytochemistry 7, 2157–2171.

McKirdy, D.M., Cox, R.E., Volkman, J.K., Howell, V.J., 1986. Botryococcane in a new class of Australian non-marine crude oils. Nature 320, 57–59.

Moldowan, J.M., Seifert, W.K., 1980. First discovery of botryococcane in petroleum. Journal of the Chemical Society, Chemical Communications 19, 912–914.

Özek, T., Demirci, F., 2012. Isolation of natural products by preparative gas chromatography. In: Satyajit, D.S., Lutfun, N. (Eds.), Methods in Molecular Biology, Natural Products Isolation. Humana Press, New York, pp. 275–300.

Philp, R.P., Lewis, C.A., 1987. Organic geochemistry of biomarkers. Annual Review of Earth and Planetary Sciences 15, 363–395.

Resch, V., Hanefeld, U., 2015. The selective addition of water. Catalysis Science & Technology 5, 1385–1399.

Rontani, J.F., Belt, S.T., Vaultier, F., Brown, T.A., 2011. Visible light induced photooxidation of highly branched isoprenoid (HBI) alkenes: significant dependence on the number and nature of double bonds. Organic Geochemistry 42, 812–822.

Rontani, J.F., Bonin, P., Vaultier, F., Guasco, S., Volkman, J.K., 2013. Anaerobic bacterial degradation of pristenes and phytenes in marine sediments does not lead to pristane and phytane during early diagenesis. Organic Geochemistry 58, 43–55.

Rontani, J.F., Belt, S.T., Vaultier, F., Brown, T., Massé, G., 2014. Autoxidation and photooxidation of highly branched isoprenoid (HBI) alkenes: a combined kinetic and mechanistic study. Lipids 49, 481–494.

Rontani, J.F., Belt, S.T., Amiraux, R., 2018. Biotic and abiotic degradation of the sea ice diatom biomarker IP_{25} and selected algal sterols in near-surface Arctic sediments. Organic Geochemistry 118, 73–88.

Rontani, J.F., Smik, L., Belt, S.T., Vaultier, F., Armbrecht, L., Leventer, A., Armand, L.K., 2019. Abiotic degradation of highly branched isoprenoid alkenes and other lipids in the water column off East Antarctica. Marine Chemistry 210, 34–47.

Schaich, K.M., 2005. Lipid oxidation: theoretical aspects. In: Shahidi, F. (Ed.), Bailey's Industrial Oil and Fat Products. sixth ed. John Wiley and Sons, New York, pp. 269–355.

Soltani, M., Metzger, P., Largeau, C., 2004. Effects of hydrocarbon structure on fatty acid, fatty alcohols and β-hydroxy acid composition in the hydrocarbon-degrading bacterium *Marinobacter hydrocarbonoclasticus*. Lipids 39, 491–505.

Schouten, S., Schoell, M., Rijpstra, W.I.C., Sinninghe Damsté, J.S., de Leeuw, J.W., 1997. A molecular stable carbon isotope study of organic matter in immature Miocene Monterey sediments, Pismo basin. Geochimica et Cosmochimica Acta 61, 2065–2082.

Swaving, J., de Bont, J.A.M., 1998. Microbial transformation of epoxides. Enzymes and Microbial Technology 22, 19–26.

Volkman, J.K., 2014. Acyclic isoprenoid biomarkers and evolution of biosynthetic pathways in green microalgae of the genus *Botryococcus*. Organic Geochemistry 75, 36–47.

Zuo, H.L., Yang, F.Q., Huang, W.H., Xia, Z.N., 2013. Preparative gas chromatography and its applications. Journal of Chromatographic Science 51, 704–715.